

# Experimental evidence for a generalized FFLO state in clean type-II superconductors with short coherence length and enhanced Pauli susceptibility

F. Steglich <sup>a,\*</sup>, R. Modler <sup>a</sup>, P. Gegenwart <sup>a</sup>, M. Deppe <sup>a</sup>, M. Weiden <sup>a</sup>, M. Lang <sup>a</sup>, C. Geibel <sup>a</sup>, T. Lühmann <sup>a</sup>, C. Paulsen <sup>b</sup>, J.L. Tholence <sup>b</sup>, Y. Ōnuki <sup>c</sup>, M. Tachiki <sup>d</sup>, S. Takahashi <sup>d</sup>

<sup>a</sup> IFP, TH Darmstadt, D-64289 Darmstadt, Germany

<sup>b</sup> CRTBT/CNRS, F-38042 Grenoble Cedex, France

<sup>c</sup> Department of Physics, Osaka University, Osaka 560, Japan

<sup>d</sup> IMR, Tohoku University, Sendai 980, Japan

## Abstract

We report an investigation of the magnetic and dilatometric properties of single crystals of the superconductors  $\text{UPd}_2\text{Al}_3$  and  $\text{CeRu}_2$ , both compounds exhibiting enhanced spin susceptibilities. Our results suggest for both systems a first-order transition between weak and strong pinning at  $T < 0.9T_c$ , somewhat below  $H_{c2}(T)$ . We argue that these observations are compatible with a staggered order parameter due to the formation of a “generalized Fulde–Ferrell–Larkin–Ovchinnikov state”.

## 1. Introduction

Tachiki et al. [1,2] have recently reported the first non-linear theory which addresses the interplay between the Abrikosov flux-line (AFL) lattice and the non-uniform superconducting Fulde–Ferrell–Larkin–Ovchinnikov (FFLO) state. In order for the latter to be created, the gain in Zeeman energy associated with the formation of generic nodal planes (the “LO planes”) perpendicular to the AFL lattice has to compensate the pay in superconducting condensation energy. For clean type-II superconductors

with short coherence length (or large Ginzburg–Landau parameter  $\kappa$ ), strong Pauli limiting and a large spin susceptibility  $\chi_s$ , a first-order transition between the AFL lattice and the FFLO state should take place and, in the presence of a weak random pinning potential, be accompanied by an abrupt change from weak to strong pinning. This can be understood as follows: Because of the large Zeeman energy, the self-energy of the vortex core is small and pinning weak. However, once the vortices become truncated by the “LO planes” at sufficiently high field, the AFL segments (with a length of several tens times the coherence length) can accommodate to the weak random pinning potential more easily than the intact vortices can at lower fields, thereby becoming efficiently pinned by the collective

---

\* Corresponding author. Fax: +49 6151 164 883;  
e-mail: dh4q@hrzpub.th-darmstadt.de.

action of weak pinning centers. This resembles the case of high-quality single crystals of the cuprate superconductor  $\text{YBa}_2\text{Cu}_3\text{O}_{7-\delta}$ : Here, an enhancement of flux pinning was observed upon approaching the melting transition of the flux lattice and was interpreted to be caused by the softening of the vortex lattice which precedes the melting [3]. Since such an increase in pinning strength gives rise to an increase in the critical-current density, it is commonly labeled ‘‘peak effect’’. In Ref. [1] comparison was made between the theoretical predictions and available results from DC magnetization and isothermal magnetostriction experiments on both the antiferromagnetically ordered heavy-fermion superconductor  $\text{UPd}_2\text{Al}_3$  ( $T_c \leq 2$  K) and the nonmagnetic strongly-intermediate-valent superconductor  $\text{CeRu}_2$  ( $T_c \leq 6.1$  K). These experimental results which highlight an anomalous peak effect for both systems were found to be qualitatively consistent with the theoretical expectation.

The present paper is aimed at providing a thorough study of single crystalline samples of both compounds. In addition to the two techniques mentioned before, results on the AC susceptibility and thermal expansion will be presented. Details concerning the crystal growth and characterization as well as the experimental set ups will be published elsewhere [4]. High-resolution length measurements on  $\text{UPd}_2\text{Al}_3$  have led to the first speculation of the occurrence of a FFLO state [5]. In Section 2, we focus on the magnetic properties of  $\text{UPd}_2\text{Al}_3$  which allow us to derive a refined  $H$ - $T$  phase diagram for this material, while Section 3 is devoted to  $\text{CeRu}_2$ . In Section 4, the results for the two compounds are put into perspective.

## 2. The antiferromagnetic heavy-fermion superconductor $\text{UPd}_2\text{Al}_3$

This hexagonal compound meets the strict requirements for the FFLO state to form at sufficiently high magnetic field [1]:

- (1) The transport mean free path  $l \approx 720$  Å greatly exceeds the Ginzburg–Landau coherence length  $\xi_0 \approx 85$  Å [6].
- (2) A large magnetic penetration depth  $\lambda_0 \approx 4000$ – $5000$  Å [6] is equivalent to a large  $\kappa = \lambda_0/\xi_0 \approx 50$ .

(3) The orbital field  $H_{c2}^*(0) \approx 61$  kϕe [1] is substantially larger than the Pauli limiting field  $H_p(0) \approx 34$  kϕe, indicating that the orbital pair breaking is sufficiently weak.

(4) The Zeeman-energy density  $\epsilon_z = 0.5\chi_s H_{c2}^2(0) = 20.6 \times 10^3$  erg/cm<sup>3</sup> ( $H \parallel c$ ) and  $16.4 \times 10^3$  erg/cm<sup>3</sup> ( $H \perp c$ ) almost coincides with  $\epsilon_c = H_{c,th}^2(0)/8\pi = 19.8 \times 10^3$  erg/cm<sup>3</sup>, the density of the superconducting condensation energy. Here, the thermodynamical critical field was estimated via  $H_{c,th}^2(0)/8\pi \approx 0.25(\gamma_0/V_{\text{mole}})T_c^2$  ( $V_{\text{mole}} = 62.94$  cm<sup>3</sup>/mole). This means likewise that the Pauli limiting field  $H_p(0)$  almost coincides with the experimental  $H_{c2}(0)$  being 32 kϕe for  $H \perp c$  and 36 kϕe for  $H \parallel c$ , respectively.

Among the heavy-fermion superconductors,  $\text{UPd}_2\text{Al}_3$  is unique in that it exhibits [7] microscopic coexistence of a superconducting condensate formed by ‘‘itinerant 5f electrons’’ (‘‘heavy fermions’’) and seemingly ‘‘more localized 5f states’’ giving rise to antiferromagnetic order below  $T_N = 14.5$  K [6]. From both Knight-shift [7] and specific-heat [8] results the ‘‘itinerant 5f subset’’ was characterized by an intrinsic Pauli susceptibility,  $\chi_p \approx 2 \times 10^{-3}$  emu/mole, and by a Sommerfeld coefficient,  $\gamma_0 \approx 125$  mJ/K<sup>2</sup>mole. These values were used in the above estimates for  $\epsilon_z$  and  $\epsilon_c$ , respectively.

Fig. 1 displays a set of DC-magnetization curves measured as a function of temperature at fixed mag-

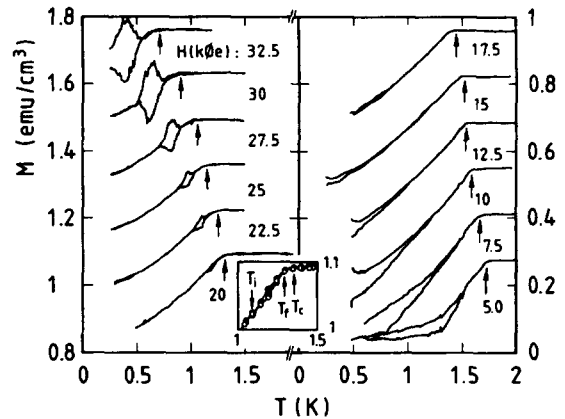


Fig. 1. ‘‘Isofield’’ DC magnetization  $M$  vs.  $T$  for different applied fields for  $\text{UPd}_2\text{Al}_3$ ,  $H \parallel [001]$ . Arrows indicate  $T_c(H)$  values. The inset shows 20 kϕe data above  $T = 1$  K: (○) and (●) denote values of the magnetization taken upon moving the sample up/down within the pick-up coils of the magnetometer.  $T_1$  and  $T_2$  mark onset and offset temperatures of the irreversibility range.

netic fields  $H$  applied along the hexagonal  $c$ -axis. The low-field data for  $H \leq 17.5$  k $\phi$ e display strong pinning at low temperature, below the irreversibility line  $H_{\text{irr}}(T)$  or  $T_{\text{irr}}(H)$ , typical for a clean type-II superconductor. Above  $T_{\text{irr}}(H)$  the magnetization is almost reversible. For magnetic fields  $H \geq 20$  k $\phi$ e, out of this almost reversible regime another irreversibility range develops somewhat below  $T_c(H)$ . This indicates an unusually strong pinning in the temperature range  $T_i \leq T \leq T_f$ , where  $T_i/T_f$  are the onset/offset temperatures of this anomalous pinning. Compared to the DC magnetization curves our AC-susceptibility traces of Fig. 2, which demonstrate enhanced diamagnetism due to strong pinning somewhat below  $T_c(H)$ , are apt to resolve this phenomenon at even lower fields (Fig. 2(b)). As seen in Fig. 2(c), the minima in the  $\chi_{\text{AC}}(T, H = \text{const})$  curves decrease linearly upon reducing the field down to 12.5 k $\phi$ e. The peaks below 10 k $\phi$ e which deviate from the straight line in Fig. 2(c) are ascribed to demagnetizing fields near the edges and corners of our UPd<sub>2</sub>Al<sub>3</sub> single crystal; thus, apparently no intrinsic anomalous peak effect occurs at lower fields ( $T > T^* \approx 1.6$  K).

In Fig. 3, we compare results, taken at  $H = 25$  k $\phi$ e along the [110] direction, for measurements of (a) the sample length  $\Delta l(T)$  and (b) the linear thermal-expansion coefficient  $\alpha(T)$  with those of (c)  $M(T)$  and (d)  $\chi_{\text{AC}}(T)$ . Figs. 3(c) and (d) demonstrate that the hysteresis loop in the DC magnetization and

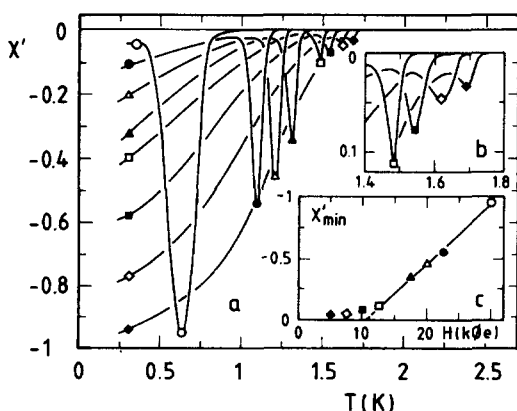


Fig. 2. Real part of  $\chi_{\text{AC}}(T, H = \text{const.})$  for UPd<sub>2</sub>Al<sub>3</sub> (a, b) at different magnetic fields as indicated by the symbols (c) which mark the magnitude of the minimum vs. the applied field.

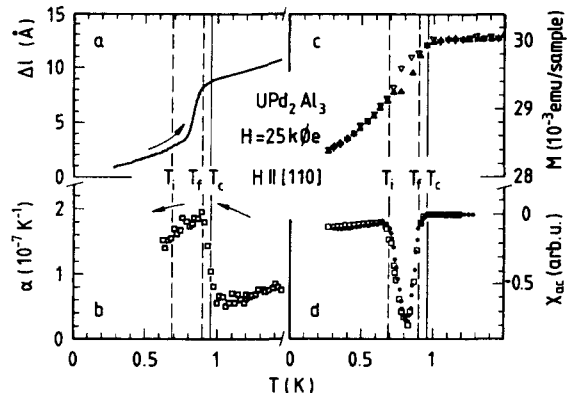


Fig. 3. Isofield ( $H = 25$  k $\phi$ e) results on UPd<sub>2</sub>Al<sub>3</sub> indicate that the sample length (a) relaxes upon warming at  $T < T_f < T_c$ .  $T_c$  is determined from the midpoint of the jump in the thermal-expansion coefficient  $\alpha(T)$ , determined in a field-cooled experiment (b). The temperatures  $T_i$  and  $T_f$  mark the onset and the offset of the strong-pinning regime as observed in  $M(T)$  (c) and  $\chi_{\text{AC}}(T)$  (d), respectively; full/open symbols denote values of the hysteretic magnetization taken upon moving the sample up/down within the pick-up coils of the magnetometer (c) and data points registered upon warming and cooling (d), respectively.

the diamagnetic peak in the AC susceptibility (at  $T_i < T < T_f$ ), both indicating extraordinary pinning, almost coincide. This temperature range is well separated from the superconducting transition temperature  $T_c$ , being determined from the midpoint of the mean-field transition in  $\alpha(T)$ , when measured upon cooling in constant field (Fig. 3(b)). The positions of  $T_i(H)$ ,  $T_f(H)$  and  $T_c(H)$  as well as of  $H_i(T)$ ,  $H_f(T)$  and  $H_{c2}(T)$ , the latter being obtained through isothermal field scans, can be used to construct the  $H$ - $T$  phase diagrams of Fig. 4. In agreement with previous results [5], these phase diagrams for  $H \perp c$  and  $H \parallel c$  make manifest a moderate anisotropy.

### 3. The paramagnetic intermediate-valence superconductor CeRu<sub>2</sub>

The cubic Laves phase compound CeRu<sub>2</sub>, too, is a clean type-II superconductor with short coherence length  $\xi_0 = 61$  Å ( $\ll l \approx 1300$  Å) and large  $\kappa \approx 16$  [9]. Like for UPd<sub>2</sub>Al<sub>3</sub>, the orbital field  $H_{c2}^*(0) \approx 118$  k $\phi$ e comfortably exceeds [1] the Pauli limiting field  $H_p(0) = (79 \pm 8)$  k $\phi$ e. Note, however, that the temperature dependence of the upper critical field ex-

hibits a striking anomaly found by several groups [4,9,10]:  $H_{c2}(T)$  shows an upturn near  $H = 10$  k $\phi$ e, and its initial slope  $-(dH_{c2}/dT)_{T_c} \approx 12$  k $\phi$ e/K is much smaller than  $\approx 26.5$  k $\phi$ e/K expected from  $H_{c2}^*(0)$ .

In order to obtain the intrinsic Pauli susceptibility  $\chi_p$  we firstly subtract from the low- $T$ , normal-state susceptibility a Curie-Weiss-type ‘‘impurity’’ contribution corresponding to, at least, 0.2 at.% ‘‘non-transformed’’  $Ce^{3+}$  ions. This yields  $\chi_0 = 2.35 \times 10^{-4}$  (in SI units). Secondly, we correct  $\chi_0$  for the diamagnetic contributions arising from both core and conduction electrons,  $\chi_{dia} = -3.5 \times 10^{-5}$  (in SI units) [9]. The resulting Pauli susceptibility  $\chi_p = \chi_0 - \chi_{dia} = 2.7 \times 10^{-4}$  (in SI units) agrees reasonably well with published data [9,10]. Assuming that the ‘‘impurity’’ contribution  $\chi_i$  is purely spin derived, we find the total low- $T$  spin susceptibility  $\chi_{spin} = \chi_p + \chi_i(T \rightarrow 0)$  to amount to  $(2.7 \pm 0.5) \times 10^{-5}$  emu/cm<sup>3</sup>. Using  $H_{c2}(0) \approx 70$  k $\phi$ e (inset of Fig. 5), we estimate a Zeeman-energy density  $\epsilon_z \approx (67 \pm 12) \times 10^3$  erg/cm<sup>3</sup>. Employing the Sommerfeld coefficient  $\gamma_0 = 29$  mJ/K<sup>2</sup>mole [9] and  $V_{mole} = 32.23$  cm<sup>3</sup>/mole, the density of the condensation energy is estimated to be  $\epsilon_c = 84 \times 10^3$  erg/cm<sup>3</sup>. This value presumably overestimates  $\epsilon_c$  substantially, since pair breaking by paramagnetic ‘‘impurities’’ (with con-

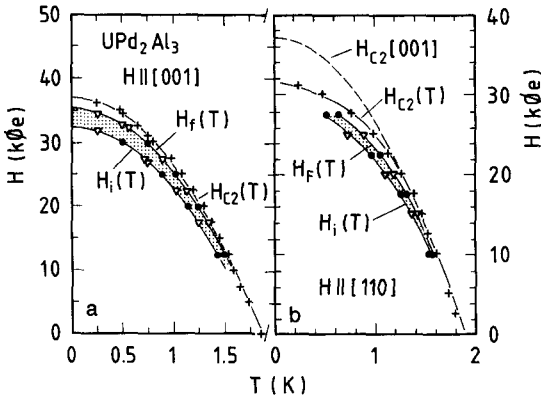


Fig. 4.  $H$ - $T$  phase diagram of  $UPd_2Al_3$  for  $H \parallel [001]$  (a) and  $H \parallel [110]$  (b). Anomalies in  $M(H, T)$  ( $\nabla$ , Fig. 1) and  $\chi_{AC}(T)$  ( $\bullet$ , Fig. 2) define onset [ $H_i(T)$ ] and offset [ $H_f(T)$ ] of irreversibilities; see text. Upper critical field  $H_{c2}(T)$  denoted by + [ $\chi_{DC}(T)$ ]. The dashed line in (b) marks  $H_{c2}(T)$  for  $H \parallel [001]$ .

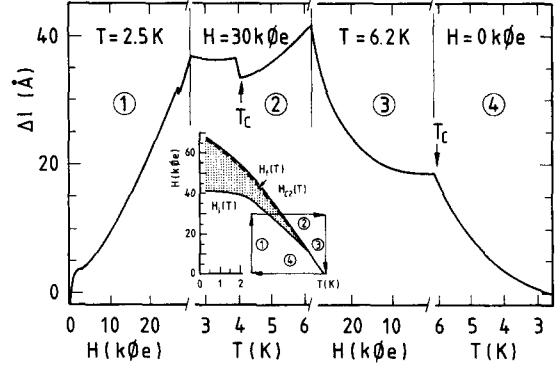


Fig. 5. Dilatometric investigation of a closed cycle in the  $H$ - $T$  plane of  $CeRu_2$  (see inset), consisting of four subsequent measurements ( $H \parallel [110]$ ): (1) isothermal magnetostriction ( $T = 2.5$  K) starting from the superconducting state after ZFC, (2) isofield thermal expansion ( $H = 30$  k $\phi$ e), (3) isothermal magnetostriction ( $T = 6.2$  K) and (4) zero-field thermal expansion. Since the length balance is conserved, the small discontinuity in run (1) may be ascribed to a jump of flux bundles within the weak-pinning superconducting state. The characteristic length jump in run (2) occurs at  $T = (3.90 \pm 0.03)$  K, i.e., below  $T_c$  ( $30$  k $\phi$ e) =  $(3.98 \pm 0.02)$  K: both the magnitude and sign of the anomaly depend strongly on the field history (1), cf. also Fig. 6.

centration  $\geq 0.2$  at.%  $Ce^{3+}$  ions) reduces the condensation energy. Future low-temperature measurements of the specific heat and magnetization on the same sample are in preparation in order to obtain more accurate estimates for  $\epsilon_z$  and  $\epsilon_c$ . Given the present uncertainty margins, the Zeeman energy density and the condensation-energy density are considered to be close to each other. Not surprisingly, several groups [9–14] reported anomalies related to an anomalous peak effect for  $CeRu_2$ , too. The experimental techniques applied in these investigations were DC magnetization, AC susceptibility, elastic constants and magnetocaloric effect.

In the following, we wish to concentrate on length measurements performed as a function of both  $T(H = \text{const.})$  and  $H(T = \text{const.})$ . Such experiments were at the heart of the initial work on  $UPd_2Al_3$  in Ref. [5]. Fig. 5 shows a typical result for a closed cycle in the  $H$ - $T$  phase diagram of  $CeRu_2$  (see inset). Two observations are worth mentioning: (1) The length balance holds over the full cycle. (2) A pronounced length change takes place along path 2 near  $T_f(H) < T_c(H)$ , whereas no anomaly can

be resolved at lower temperatures, i.e. when warming the sample to  $T \geq T_i(H)$ . This discontinuous change in  $\Delta l$  near  $T = T_i$  corresponds to the one for  $\text{UPd}_2\text{Al}_3$  displayed in Fig. 3(a) and indicates a pronounced relaxation of the sample length. The latter occurs slightly above the temperature of maximum pinning (cf. Figs. 3(c) and (d)). For  $\text{UPd}_2\text{Al}_3$ , too, no anomaly can be resolved in the corresponding experiment at  $T = T_i$  where the transition takes place from weak to strong pinning. At first glance, this is a counter-intuitive result which, however, finds a natural explanation in the fact that in the  $\Delta l(T, H = \text{const.})$  measurement there is no driving force acting on the flux lines:

- (1) Because of the high  $\kappa$ , the high-field magnetization, i.e. the concentration of vortices, does virtually not change upon warming.
- (2) In the absence of temporal field variations, no Lorentz force is operative which would enable the AFL lattice to gain energy by taking advantage of the strong pinning at  $T \geq T_i$ . On the other hand, in the measurements of both DC magnetization (due to the motion of the sample along a small field gradient) and, of course, AC susceptibility the Lorentz force is operative, and the abrupt increase in pinning

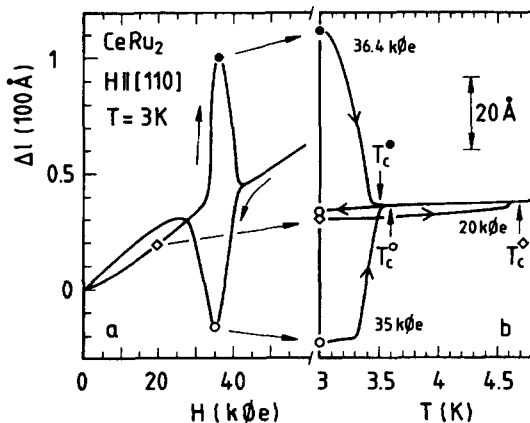


Fig. 6.  $\text{CeRu}_2$ : Isothermal magnetostriction  $\Delta l$  vs.  $H$  (a) and length change  $\Delta l$  vs.  $T$  measured upon warming at different fields (b), starting from different points of the isothermal  $\Delta l(H)$  curve displayed in (a).  $\Delta l(T)$  data are shifted in order to coincide with the normal-state value. Field-cooled curve  $\Delta l(T)$  is shown for  $H = 35$  kOe only.

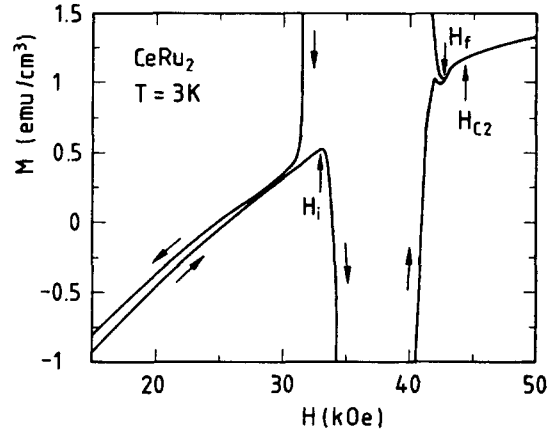


Fig. 7. Isothermal DC magnetization  $M$  vs.  $H$  of  $\text{CeRu}_2$  at  $T = 3$  K. Arrows indicate measurements done on increasing and reducing the field, respectively, as well as onset ( $H_i$ ), offset ( $H_f$ ) fields of strong-pinning regime and upper critical field ( $H_{c2}$ ). In agreement with the magnetostriction results (Fig. 6), the magnetization is not strictly reversible below  $H = H_i$ .

strength can be easily recognized. The above reasoning that  $\Delta l(T, H = \text{const.})$  does not react on the prominent first-order transition when warming the sample to  $T \geq T_i$  presumes a non-equilibrium state, i.e. the existence of a finite pinning potential, already in the seemingly “reversible” regime ( $T < T_i$ ). In fact, hysteresis effects in this part of the  $H$ - $T$  phase diagram are clearly resolved in the magnetostriction data,  $\Delta l(H, T = \text{const.})$ , of Fig. 6(a) and in the isothermal DC-magnetization curves,  $M(H, T = \text{const.})$ , of Fig. 7. Note that no hysteresis is seen in these experiments above  $H = H_i$ ;  $H_i$  being the depinning field at which the intervortex interaction eventually exceeds the pinning force, so that the pinning centers become inefficient.

Compared to the  $\text{UPd}_2\text{Al}_3$  data [1,4], the magnetization results for  $\text{CeRu}_2$  displayed in Fig. 7 exhibit a more abrupt increase of the diamagnetic response upon increasing the field to  $H \geq H_i$ . Along with the paramagnetic peak showing up on decreasing the field, this anomaly proves the existence of shielding currents due to trapped flux inside the superconductor. The sudden onset of strong pinning at  $H_i$  and the hysteresis of  $H_i$  on increasing/decreasing the field indicate that this transition is, in fact, of first order.

Further support for our claim that in  $\text{CeRu}_2$  a strongly pinned vortex state exists above  $H_1$  derives from pronounced magnetostriction anomalies: Fig. 6(a) shows the field-induced length change measured under isothermal conditions at  $T = 3$  K. These data clearly demonstrate that the coupling of the vortex lattice to the crystal lattice increases the stronger the pinning: the abrupt change from weak to strong pinning when increasing the field to  $H \geq H_1$  causes an enormous increase in the stress, induced by the trapped vortices that act on the sample. The amplitude of the magnetostriction anomaly is found to be precipitously reduced upon warming the sample, eventually disappearing completely at  $T > T^* \approx 5.4$  K (corresponding to  $H < H^* \approx 10$  k $\phi$ e). Very similar  $\Delta l(H, T = \text{const})$  results for  $\text{UPd}_2\text{Al}_3$  are reported in Ref. [5].

Returning to the relaxation of the sample length (upon warming) that gives rise to a step-like change in  $\Delta l(T, H = \text{const})$ , we wish to note that, like for  $\text{UPd}_2\text{Al}_3$  [5], different signs for these quasi-discontinuous length changes can be observed in different runs on the same sample. The  $\text{CeRu}_2$  data of Fig. 6(b) reveal that both the size and sign of this length jump depend on the field history, i.e. the way by which the magnetic field was applied to the sample (Fig. 6(a)), following an initial zero-field cooling.

#### 4. Perspective

We have found similar anomalies in the magnetic and dilatometric properties, indicating highly unusual pinning properties, for two otherwise very different superconductors, the antiferromagnetically ordered heavy-fermion compound  $\text{UPd}_2\text{Al}_3$  and the nonmagnetic intermediate-valence compound  $\text{CeRu}_2$ . Our experimental results resemble the well-known peak effect in type-II superconductors. However, we feel that we can discard the conventional causes giving rise to a peak effect in these two compounds:

- (1) Sample inhomogeneities implying normal regions of mesoscopic size [15] are unlikely in view of both the good sample quality [4] and of the almost reversible magnetization curves at  $H < H_1$ ;
- (2) a “matching effect” between the array of pinning centers and the AFL lattice would have to occur for the same  $H$  field almost independent of  $T$ , and

no peak effect should be observed in temperature scans at  $H = \text{const}$  [16], in contrast to our observations;

- (3) a “synchronization”, i.e. a softening of the AFL lattice overcompensating the weakening of the pinning force upon increasing  $H$  [17] should result in a gradual rather than in an abrupt increase in pinning. In addition, “synchronization” should work close to  $T_c$  (close to  $H = 0$  k $\phi$ e), while the anomalies observed experimentally are confined to  $H > H^* = 10$  k $\phi$ e.

(4) The latter holds true also for the first-order transition between weak and strong collective pinning found in amorphous  $\text{Nb}_3\text{Ge}$  and  $\text{Mo}_3\text{Si}$  films and ascribed to a three- to two-dimensional crossover of the AFL lattice [18].

Therefore, our observations highlight a peak effect of novel origin.

Several points deserve further consideration:

- (1) In order to observe the formation of the FFLO state via the anomalous peak effect, a suitable random pinning potential is required. If the pinning is too strong, an irreversible magnetization curve in the whole Shubnikov phase may be observed, as, e.g., in  $\text{CeCu}_2\text{Si}_2$  [19]. On the other hand, in a nearly homogeneous type-II superconductor, the magnetization curve may be almost reversible in the whole mixed state. There is evidence that extremely high-quality single crystals of  $\text{UPd}_2\text{Al}_3$  come close to this clean limit [20]. Comparison of the DC-magnetization results of Figs. 1 and 7 suggest substantially stronger pinning centers to exist in  $\text{CeRu}_2$  than in  $\text{UPd}_2\text{Al}_3$ . In this context the role of pair-breaking paramagnetic  $\text{Ce}^{3+}$  “impurities”, found evidence for by a Curie-Weiss contribution to the susceptibility of  $\text{CeRu}_2$ , has to be explored by future experiments.

- (2) The origin of the unique jump in the length, measured upon warming the sample as a function of temperature at constant field ( $H > 10$  k $\phi$ e), is not fully understood. As seen in Fig. 4, (the midpoint of) this anomaly occurs intermediate between the temperature of maximum pinning and  $T_f(H)$ , the depinning temperature. We relate this anomaly to a pronounced weakening of the pinning force within a rather narrow temperature window. Future calculations have to show in which way  $T$ -dependent changes of the modulated order parameter are essential for this rapid reduction in the pinning force.

(3) Compared to the original theories [21,22] which assume an isotropic order parameter and restrict the FFLO state to  $T < 0.56T_c$ , we find for both UPd<sub>2</sub>Al<sub>3</sub> and CeRu<sub>2</sub> a greatly enhanced existence range,  $T < 0.9T_c$ . In addition, the existence range of the FFLO state on the field axis is, especially for CeRu<sub>2</sub>, much wider than expected in Refs. [21] and [22], which assume spherical Fermi surfaces. In contrast to this assumption, both UPd<sub>2</sub>Al<sub>3</sub> [23] and CeRu<sub>2</sub> [24] exhibit complex Fermi surfaces with almost disjunct portions. Thus, an antiferromagnetic exchange interaction among electronic quasiparticles is probable, which should favor an expanded field range for the FFLO state [25]. In fact, for CeRu<sub>2</sub> we estimate a Sommerfeld–Wilson ratio  $R \approx 0.8$ , which yields a Landau parameter  $F_0^s \approx +0.25$  [4]. An improved theory should, therefore, incorporate realistic band structures.

We conclude by stating that, although the aforementioned problems need to be solved by further theoretical and experimental research, the proposal by Tachiki et al. [1] of a staggered order parameter due to the formation of a generalized FFLO state provides a natural explanation for the sudden change from weak to strong pinning in UPd<sub>2</sub>Al<sub>3</sub> as well as CeRu<sub>2</sub>. Four necessary, but not sufficient, conditions for the occurrence of those unique pinning anomalies have been derived:

- (1) a large electronic mean free path,
- (2) a short superconducting coherence length,
- (3) strong Pauli limiting and
- (4) a large spin susceptibility of the normal metal.

In addition, a suitable random pinning potentials appears to be required.

These criteria should enable one to find further FFLO superconductors, notably among the heavy-fermion compounds; UBe<sub>13</sub> [26] and UPt<sub>3</sub> [27] being prime candidates. The case of CeRu<sub>2</sub> shows, however, that the FFLO state can also form in conventional superconductors for which it had been proposed some three decades ago [21,22]. Further examples may be found among the A15 [28] and borocarbide [29] superconductors. Another line of future research activities should focus on the decoration of the unique nodal structure of the staggered FFLO order parameter. Such experiments may include neutron scattering with non-magnetic systems like CeRu<sub>2</sub> and scanning-vacuum-tunneling spectroscopy.

## Acknowledgements

The authors are grateful to P. Fulde, T. Fujita, K. Gloos, A.D. Huxley, K. Kadowaki, M.B. Maple and D. Rainer for valuable discussions. They are indebted to N. Sato and T. Komatsubara for providing the UPd<sub>2</sub>Al<sub>3</sub> single crystal. This work was supported by the SFB 252 Darmstadt/Frankfurt/Mainz.

## References

- [1] M. Tachiki et al., Z. Phys. B, to be published.
- [2] M. Tachiki et al.; S. Takahashi et al. (these proceedings).
- [3] W.K. Kwok et al., Phys. Rev. Lett. 73 (1994) 2614.
- [4] R. Modler et al., Phys. Rev. Lett. 76 (1996) 1292.
- [5] R. Modler et al., Int. J. Mod. Phys. B 7 (1993) 42; K. Gloos et al., Phys. Rev. Lett. 70 (1993) 501.
- [6] C. Geibel et al., Z. Phys. B 84 (1991) 1; A. Amato et al., Europhys. Lett. 19 (1992) 127.
- [7] R. Feyerherm et al., Phys. Rev. Lett. 73 (1994) 1849.
- [8] F. Steglich et al., Proc. Int. Conf. on High Magnetic Fields, Tallahassee (1995), to be published.
- [9] A.D. Huxley et al., J. Phys. Condens. Mat. 5 (1993) 7709.
- [10] K. Kadowaki et al., (preprint 1995).
- [11] K. Yagasaki et al., J. Phys. Soc. Jpn. 62 (1993) 3825.
- [12] Cf. also: S.B. Roy and B.R. Coles, J. Condens. Mat. 6 (1994) L 663; H. Sugawara et al., Physica B 206&207 (1993) 196; M.B. Maple, private communication.
- [13] H. Goshima et al. Physica B 206&207 (1995) 193.
- [14] H. Goshima et al., Physica B, to be published.
- [15] See, e.g.: W. Buckel, Supraleitung (VHC, Weinheim, 1990).
- [16] A.M. Campbell and J.E. Evetts, Adv. Phys. 21 (1972) 90.
- [17] A.B. Pippard, Philos. Mag. 19 (1969) 217.
- [18] R. Wördenweber and P.H. Kes, Cryogenics 29 (1989) 321.
- [19] P. Gegenwart, Diploma Thesis, TH Darmstadt (1994) (unpublished); R. Modler, Dissertation, TH Darmstadt (1995) (unpublished).
- [20] N. Sato, private communication.
- [21] P. Fulde and R.A. Ferrell, Phys. Rev. 135 (1964) 550.
- [22] A.I. Larkin and Yu.N. Ovchinnikov, Zh. Eksp. Teor. Fiz. 47 (1964) 1136.
- [23] Experiment: Y. Inada et al., Physica 206&207 (1995) 33; Theory: L.M. Sandratskii et al., Phys. Rev. B 50 (1994) 15834.
- [24] M. Hedo et al., J. Phys. Soc. Jpn., to be published.
- [25] H. Burkhardt and D. Rainer, Ann. Physik 3 (1994) 181.
- [26] F. Thomas et al., J. Low Temp. Phys. 102 (1996) 117.
- [27] K. Tenya et al. (preprint 1995).
- [28] M. Ishino et al., Phys. Rev. B 38 (1988) 4457.
- [29] K. Kadowaki, private communication.